Dynamic analysis for a circular lined tunnel with an imperfectly bonded interface impacted by plane SH-waves

C. Yi, P. Zhang, D. Johansson and U. Nyberg
Division of Mining and Geotechnical Engineering, Luleå University of Technology, Luleå, Sweden.

ABSTRACT: The analytic solutions for the dynamic response of a circular lined tunnel with an imperfectly bonded interface subjected to plane SH-waves are presented in the paper. Wave function expansion method was used and the imperfect interface was modeled with a linear spring model. The case that the rock is harder than the liner and the case that the rock is softer than the liner were investigated. The results showed that the low frequency incident wave leads to the higher dynamic stress concentration factor (DSCF) than the high frequency incident wave. When the rock is harder than the liner, the variation of spring stiffness has more apparent effect on the DSCF in the rock for the high frequency incident wave than for the low frequency incident wave. The variations of DSCF in rock with different frequencies of incident wave and different spring stiffnesses were also discussed. When the bond is extremely weak, the resonance scattering phenomena can be observed.

1 INTRODUCTION

Underground structures are used for a variety of purposes in many areas such as transportation, mining, caverns for powerhouses and so on. Although it was a common notion that underground structures such as tunnels generally performed better than above ground structures during earthquakes, some underground structures have undergone severe damages during earthquakes. In order to provide the safe condition during an earthquake, the support systems of underground facilities, such as tunnel linings, are usually designed to withstand both static overburden and seismic loading. The study of response of lined tunnels and pipelines to dynamic loading is a fundamental engineering problem.

Extensive efforts have been dedicated to studying the dynamic response of lined or unlined tunnels. Pao and Mow (1973) used the wave function expansion method to study the dynamic response of lined tunnel in a homogeneous medium. Lee and Trifunac (1979) investigated the seismic response of a lined tunnel under incident SH wave in a half space by studying twin tunnels in a full space using co-ordinate transform technique. Shi et al. (1996) investigated the interaction of plane SH waves and a non-circular cavity with an elastic lining in an anisotropic medium using the conformal mapping method together with the wave function expansion method. Kattis et al. (2003) studied 2D dynamic response of unlined and lined tunnels in poroelastic soil to harmonic body waves. Dynamic response of twin lined tunnels buried in an infinite medium and subjected to seismic loadings was investigated by Moore and Guan (1996) using the successive reflection method. Hasheminejad et al. (2008) presented an exact analysis for three dimensional dynamic interactions of monochromatic seismic plane waves with two lined circular parallel tunnels within a boundless fluid-saturated porous elastic medium. Atymtayeva et al (2012) dealt with the diffraction of elastic PP-, SV- and SH- waves on the arbitrary deep-founded cavities in the anisotropic rock massif.

Generally, the interface between the tunnel and the liner is treated as perfectly bonded in previous studies, which means that the traction and displacement on the interface are

continuous. In practice, interface bonding is often imperfect because of the presence of microcracks or interstitial media in the interface. In this paper, the primary goal is to study the effects of interface behavior between tunnel surface and liner on the dynamic response of lined tunnels under incident SH-waves using wave function expansion method and modeling the imperfect bonded interface with a spring model.

2 GOVERNING EQUATIONS

We consider an infinitely long lined circular tunnel of outer radius b and inner radius a in rock mass. A plane harmonic SH-wave propagates in the rock mass in the positive x-direction and meets the lined tunnel, see Fig.1. The SH-wave can be expressed as in Eq. (1) (Pao and Mow, 1973).

$$\phi^{(i)} = \varphi_0 e^{i(\beta_1 x - \omega t)} \tag{1}$$

where $\phi^{(i)}$ is the incident SH-wave, φ_0 is the amplitude of the incident wave, i is the unit of complex, β_1 is the wave number of the SH-wave in the rock mass, t is time. $\omega = 2\pi f$ is the circular frequency of the incident SH-wave and f is the frequency of the incident SH-wave.

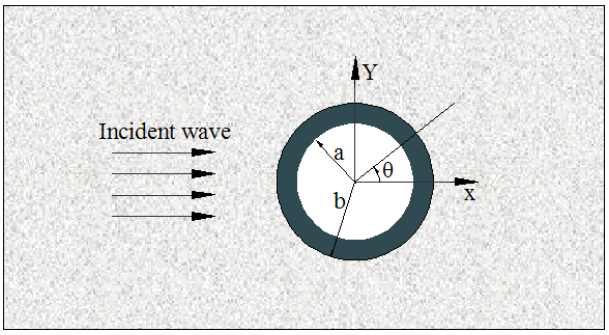

Figure.1. Problem geometry.

According to the wave function expansion method, Eq. (1) can be written as:

$$\phi^{(i)} = \varphi_0 \sum_{n=0}^{\infty} \varepsilon_n (i)^n J_n(\beta_1 r) \cos n\theta e^{-i\omega t} \tag{2}$$

where J_n is the Bessel function in n order, $\varepsilon_0 = 1$ and $\varepsilon_n = 1$ when $n \geq 1$.

When the incident SH-wave meets the circular lined tunnel, there is a reflected SH-wave ($\psi_1^{(r)}$) in rock mass from the interface between the tunnel and the liner. It can be expressed as Eq. (3):

$$\psi_1^{(r)} = \varphi_0 \sum_{n=0}^{\infty} A_n H_n^{(1)}(\beta_1 r) \cos n\theta e^{-i\omega t} \tag{3}$$

where A_n is an uncertain constants and $H_n^{(1)}$ is the first kind of Hankel function in n order, which represents the outward-propagating cylindrical wave.

There is a reflected wave in liner which propagates outwards from the inside boundary of the liner. It is a reflected SH-wave ($\psi_2^{(r)}$) and can be expressed as Eq. (4):

$$\psi_2^{(r)} = \varphi_0 \sum_{n=0}^{\infty} B_n H_n^{(1)}(\beta_2 r) \cos n\theta e^{-i\omega t} \tag{4}$$

where β_2 is the wave number of SH-wave in the liner and B_n is an uncertain constant.

There is an SH-wave ($\psi_3^{(r)}$) that propagates to the inside of liner from the outside boundary of liner. It can be expressed as Eq. (5):

$$\psi_3^{(r)} = \varphi_0 \sum_{n=0}^{\infty} C_n H_n^{(2)}(\beta_2 r) \cos n\theta e^{-i\omega t} \tag{5}$$

where $H_n^{(2)}$ is the second kind of Hankel function in n order, which represents an inwards-propagating cylindrical wave. C_n is an uncertain constant.

The total wave in rock mass can be expressed as Eq. (6):

$$\psi^{(t1)} = \varphi_0 \sum_{n=0}^{\infty} [\varepsilon_n i^n J_n(\beta_1 r) + A_n H_n^{(1)}(\beta_1 r)] \cos n\theta e^{-i\omega t} \tag{6}$$

The total wave in liner can be expressed as Eq. (7):

$$\psi^{(t2)} = \varphi_0 \sum_{n=0}^{\infty} [B_n H_n^{(1)}(\beta_2 r) + C_n H_n^{(2)}(\beta_2 r)] \cos \theta e^{-i\omega t} \tag{7}$$

Here, there are three uncertain constants, which can be obtained by help of boundary conditions.

3 BOUNDARY CONDITIONS

The state of liner bonding condition strongly affects the overall dynamic response of a tunnel. Usually, the rock mass and the liner are assumed to be bonded perfectly. But as aforementioned, sometimes the bond may be imperfect. Several imperfect interface models were proposed (Jones and Whittier, 1967;

Murty, 1975; Newmark et al., 1951; Paskaramoorthy et al., 1988; Rokhlin and Wang, 1991). Reviews of interface conditions in elastic wave problems have been presented by Martin (1992), Huang et al. (1997) and Wang et al. (2000). In the present work, the spring model is adopted to model the imperfect interface. The spring model is one of the popular models for modeling the imperfect interface (Achenbach and Zhu, 1989; Shen et al., 2001; Sudak et al., 1999; Valier-Brasier et al., 2012). The model assumes that tractions are continuous but displacements are discontinuous across the interface. In particular, the model assumes that the tractions are proportional to the corresponding displacement discontinuities through stiffness parameters. Using this concept, the boundary conditions to be applied at the interface of the liner and the rock mass can be described as Eq. (8).

$$\left.\begin{aligned} u_{z1}-u_{z2}&=\frac{\sigma_{rz1}}{k_s}\\ \sigma_{rz1}&=\sigma_{rz2}\end{aligned}\right\} \tag{8}$$

where k_s is tangential spring stiffness. The subscripts of 1 and 2 denote the components in rock and liner, respectively.

At the inner boundary of liner, the boundary condition can be expressed as Eq. (9):

$$\sigma_{rz2}=0 \tag{9}$$

4 STRESSES AND DISPLACEMENTS IN THE ROCK AND THE LINER

We omit the time factor of $e^{-i\omega t}$. The relation between displacement and stress can be expressed as,

$$\sigma_{rz}=\mu\frac{\partial u_z}{\partial r}\qquad \sigma_{\theta z}=\mu\frac{1}{r}\frac{\partial u_z}{\partial\theta} \tag{10}$$

Displacement in rock mass can be expressed as Eq. (11):

$$u_{z1}=\varphi_0\sum_{n=0}^{\infty}[\varepsilon_n i^n J_n(\beta_1 r)+A_n H_n^{(1)}(\beta_1 r)]\cos n\theta \tag{11}$$

Stress in rock mass can be expressed as Eq. (12)

$$\left\{\begin{aligned}\sigma_{rz1}&=\mu_1\frac{\varphi_0}{r}\sum_{n=0}^{\infty}[\varepsilon_n i^n[nJ_n(\beta_1 r)-\beta_1 rJ_{n+1}(\beta_1 r)]\\&\quad+A_n[nH_n^{(1)}(\beta_1 r)-\beta_1 rH_{n+1}^{(1)}(\beta_1 r)]]\cos n\theta\\ \sigma_{\theta z1}&=-\mu_1\frac{\varphi_0}{r}\sum_{n=0}^{\infty}n[\varepsilon_n i^n J_n(\beta_1 r)\\&\quad+A_n H_n^{(1)}(\beta_1 r)]\sin n\theta\end{aligned}\right. \tag{12}$$

Displacement in liner can be expressed as Eq. (13):

$$\psi^{(t2)}=\varphi_0\sum_{n=0}^{\infty}[B_n H_n^{(1)}(\beta_2 r)+C_n H_n^{(2)}(\beta_2 r)]\times\cos n\theta e^{-i\omega t} \tag{13}$$

Stress in the liner can be expressed as Eq. (14):

$$\left\{\begin{aligned}\sigma_{rz2}&=\mu_2\frac{\varphi_0}{r}\sum_{n=0}^{\infty}[B_n[nH_n^{(1)}(\beta_2 r)-\beta_2 rH_{n+1}^{(1)}(\beta_2 r)]\\&\quad+C_n[nH_n^{(2)}(\beta_2 r)-\beta_2 rH_{n+1}^{(2)}(\beta_2 r)]\cos n\theta\\ \sigma_{\theta z2}&=-\mu_2\frac{\varphi_0}{r}\sum_{n=0}^{\infty}n[B_n H_n^{(1)}(\beta_2 r)\\&\quad+C_n H_n^{(2)}(\beta_2 r)]\sin n\theta\end{aligned}\right. \tag{14}$$

where μ_1,μ_2 are respective shear modulus of rock mass and liner.

According to the boundary conditions of Eq. (8) and Eq. (9), Eq. (15) can be got,

$$\begin{pmatrix}\zeta^{(11)}&\zeta^{(12)}&\zeta^{(13)}\\ \zeta^{(21)}&\zeta^{(22)}&\zeta^{(23)}\\ \zeta^{(31)}&\zeta^{(32)}&\zeta^{(33)}\end{pmatrix}\begin{pmatrix}A_n\\B_n\\C_n\end{pmatrix}=\begin{pmatrix}\zeta^{(1)}\\\zeta^{(2)}\\\zeta^{(3)}\end{pmatrix} \tag{15}$$

where

$$\zeta^{(11)}=H_n^{(1)}(\beta_1 b)-\frac{\mu_1}{k_s b}[nH_n^{(1)}(\beta_1 b)-\beta_1 bH_{n+1}^{(1)}(\beta_1 b)]$$

$$\zeta^{(12)}=-H_n^{(1)}(\beta_2 b)\qquad \zeta^{(13)}=-H_n^{(2)}(\beta_2 b)$$

$$\zeta^{(21)}=\overline{\mu}[nH_n^{(1)}(\beta_1 b)-\beta_1 bH_{n+1}^{(1)}(\beta_1 b)]$$

$$\zeta^{(22)}=-[nH_n^{(1)}(\beta_2 b)-\beta_2 bH_{n+1}^{(1)}(\beta_2 b)]$$

$$\zeta^{(23)}=-[nH_n^{(2)}(\beta_2 b)-\beta_2 bH_{n+1}^{(2)}(\beta_2 b)]$$

$$\zeta^{(32)}=nH_n^{(1)}(\beta_2 a)-\beta_2 aH_{n+1}^{(1)}(\beta_2 a)$$

$$\zeta^{(33)}=nH_n^{(2)}(\beta_2 a)-\beta_2 aH_{n+1}^{(2)}(\beta_2 a)$$

$$\zeta^{(1)}=\varepsilon_n i^n[\frac{\mu_1}{k_s b}[nJ_n(\beta_1 b)-\beta_1 bJ_{n+1}(\beta_1 b)]-J_n(\beta_1 b)]$$

$$\zeta^{(2)}=-\overline{\mu}\varepsilon_n i^n[nJ_n(\beta_1 b)-\beta_1 bJ_{n+1}(\beta_1 b)]$$

$$\zeta^{(31)}=0\qquad \zeta^{(3)}=0$$

where $\overline{\mu} = \mu_1 / \mu_2$ is the ratio of shear modulus of rock mass and liner.

5 NUMERICAL RESULTS AND DISCUSSIONS

Dynamic effects on lined tunnels are in the form of stress concentrations or deformations that they experience during earthquakes. It is important to solve the dynamic stress concentration factor (DSCF) in the tunnel and the liner under incident SH-wave. On this problem the main task is to study the DSCF in the rock mass and the edge of the liner. The DSCF $\tau^*_{\theta z}$ can be expressed as Eq. (16):

$$\tau^*_{\theta z} = \left|\tau_{\theta z} / \tau_0\right| \quad \text{where} \quad \tau_0 = \mu_1 \beta_1 \varphi_0 \tag{16}$$

To get a general solution, some dimensionless parameters are defined. Two groups of dimensionless parameters are given in Table 1. Case I can be regarded as a concrete liner structure in rock, and Case Ⅱ is a steel liner structure in rock. Three sets of dimensionless spring stiffnesses are given as shown in Table 1. The value of b/a is 1.2.

Table 1. Value of dimensionless parameters.

	Case Ⅰ	Case Ⅱ
β_2 / β_1	1.50	0.70
μ_1 / μ_2	2.90	0.31
K_s	$10.0\mu_1 / b$	$10.0\mu_1 / b$
	$1.0\mu_1 / b$	$1.0\mu_1 / b$
	$0.1\mu_1 / b$	$0.1\mu_1 / b$

The distributions of DSCF for Case I and Case II are shown in Figure 2 and Figure 3, respectively. For Case I, when the frequency of incident wave is low, the maximum of DSCF is at θ=π/2 and 3/2π in the rock and the liner, see Figure 2(a) and Figure 2(b). Increasing spring stiffness leads to slightly decreasing DSCF in the rock and increasing DSCF in the liner. When the frequency of incident wave is high, the distribution of DSCF is complicated both in the rock and the liner, see Figure2(c) and Figure 2(d). The spring stiffness of $K_s = 0.1\mu_1 / b$ leads to the smallest DSCF in the rock and the largest DSCF in the liner compared to the spring stiffness of $K_s = 1.0\mu_1 / b$ and $K_s = 10.0\mu_1 / b$. The comparison of Figure 2(a) and Figure 2(c) shows that the low frequency incident wave leads to the bigger DSCF in the rock than the high frequency incident wave.

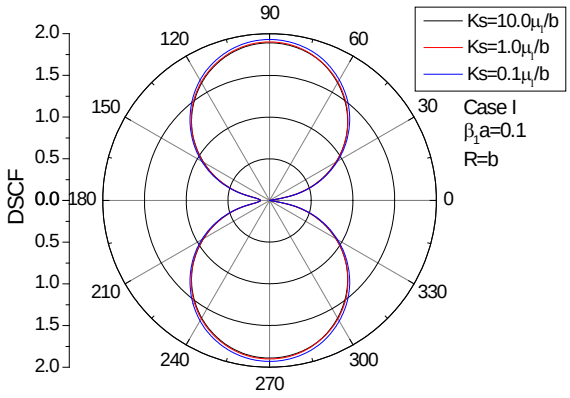

(a) DSCF in the rock

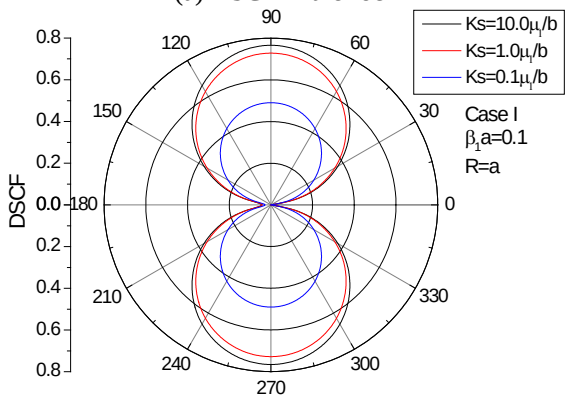

(b) DSCF in the liner

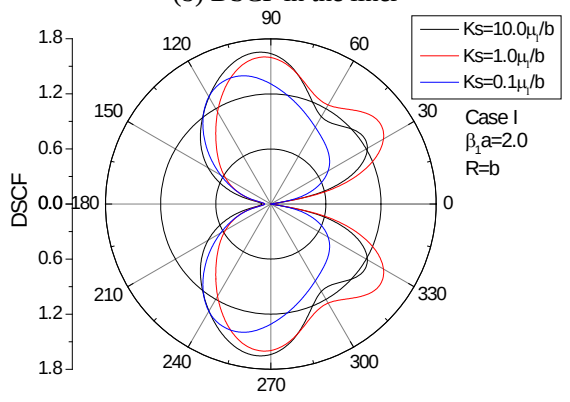

(c) DSCF in the rock

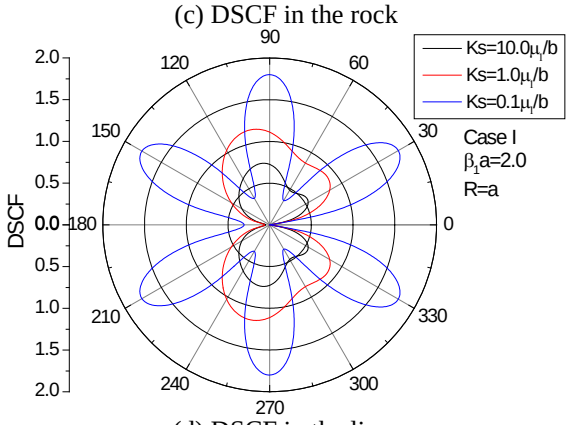

(d) DSCF in the liner

Figure 2. DSCF in the rock and liner for Case I.

For Case II, when the frequency of incident wave is low, the maximum of DSCF is at θ=π/2 and 3/2π in the rock and the liner, which is same to the Case I, see Figure 3(a) and Figure 3(b). Increasing spring stiffness leads to decreasing DSCF in the rock and increasing DSCF in the liner. When the frequency of incident wave is high, the distribution of DSCF is complicated both in the rock and the liner, see Figure 3(c) and Figure 3(d). The spring stiffness of $K_s = 0.1\mu_1 / b$ leads to the largest DSCF in the rock and the least DSCF in the liner compared to the spring stiffness of $K_s = 1.0\mu_1 / b$ and $K_s = 10.0\mu_1 / b$. The spring stiffness of $K_s = 1.0\mu_1 / b$ leads to the largest DSCF in the liner compared to $K_s = 0.1\mu_1 / b$ and $K_s = 10.0\mu_1 / b$.

The comparison of the results of Case I and Case II indicates that the stiff liner is better to reduce the DSCF in the rock than the soft liner.

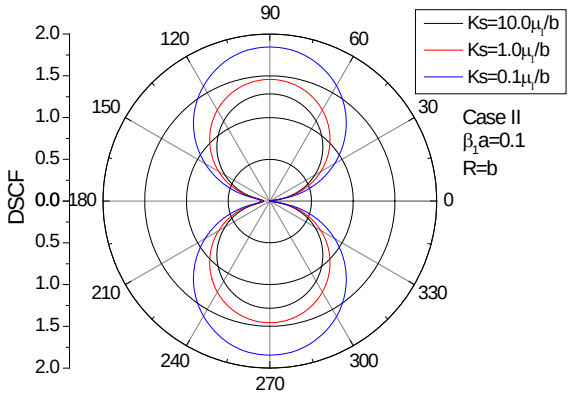

(a) DSCF in the rock

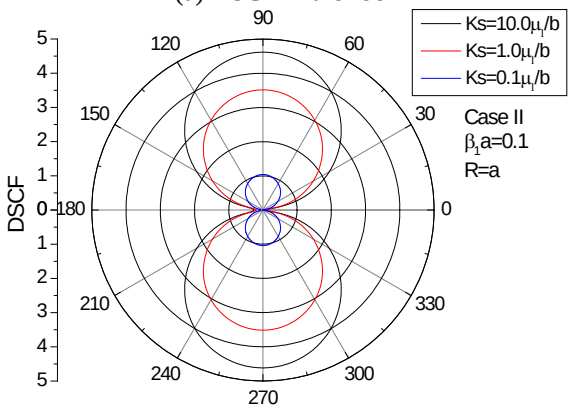

(b) DSCF in the liner

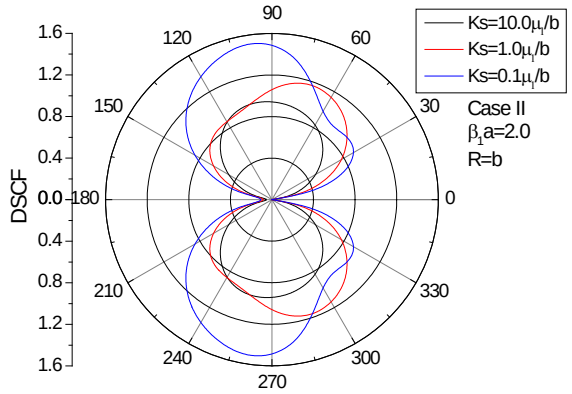

(c) DSCF in the rock

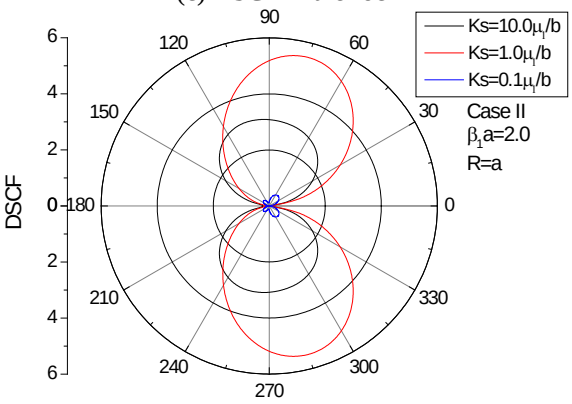

(d) DSCF in the liner

Figure 3. DSCF in the rock and liner for Case II.

The variations of DSCF in rock at $\theta=\pi$ with the change of incident wave's frequency for both cases are shown in Figure 4. The effect of variation of spring stiffness on the DSCF in the rock is more significant for Case II than for Case I, see Figure 4(a) and Figure 4(b). When the bond is extremely imperfect ($K_s = 0.1\mu_1 / b$), the results show that there are several peak values of DSCF in the rock, which is due to the resonance scattering as observed by Rajabi et al. (2009). This phenomenon is very unique for the case of the extremely imperfect interface (Wang and Sudak, 2007). When the bond is good ($K_s = 10.0\mu_1 / b$), the maximum of DSCF in rock is at $\beta_1 a = 0.40$ for Case I and at $\beta_1 a = 0.42$ for Case II.

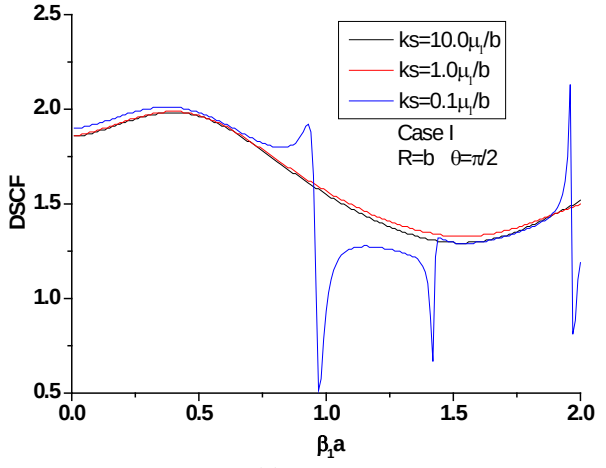

(a) Case I

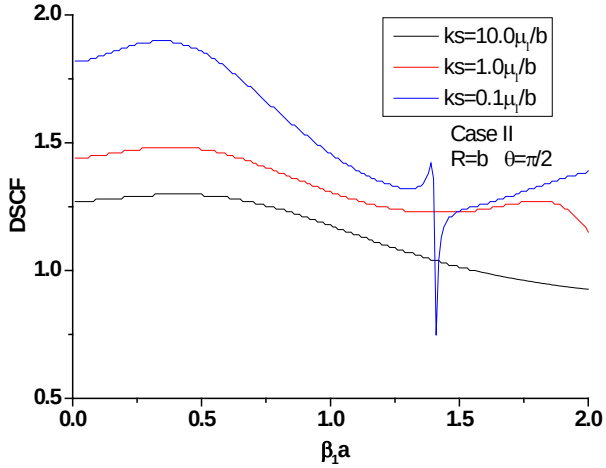

(b) Case II

Figure 4. DSCF in the rock versus the frequency of incident wave at $\theta=\pi/2$.

6 CONCLUSIONS

The influence of the boundary imperfections on the dynamic response of a lined tunnel under incident SH-waves was studied by using wave function expansion method and the spring model for the imperfect interface. The distribution of DSCF around the lined tunnel and the variation of DSCF with the change of the frequency of incident wave were presented. The results show that the boundary imperfections have different effects on the dynamic response of the lined tunnel to the low frequency and the high frequency incident waves. When the bond is extremely weak, the phenomenon of resonance scattering can be found, which can induce a large DSCF in the rock mass.

REFERENCES

Achenbach, J., Zhu, H., 1989. Effect of interfacial zone on mechanical behavior and failure of fiber-reinforced composites. *Journal of the Mechanics and Physics of Solids*,v.37, p.381-393.

Atymtayeva, L.B., Masanov, Z.K., Yagaliyeva, B.E., 2012. Diffraction of Elastic PP-, SV-and SH-Waves on the Arbitrary Deep-founded Cavities in the Anisotropic Rock Massif, In: *Proceedings of the World Congress on Engineering*. London.

Hasheminejad, S.M., Avazmohammadi, R., 2008. Dynamic stress concentrations in lined twin tunnels within fluid-saturated soil. *Journal of engineering mechanics*, 134, p.542-554.

Huang, W., Rokhlin, S., Wang, Y., 1997. Analysis of different boundary condition models for study of wave scattering from fiber–matrix interphases. The *Journal of the Acoustical Society of America*, 101, p.2031- 2042.

Jones, J., Whittier, J., 1967. Waves at a flexibly bonded interface. *Journal of Applied Mechanics*,v.34, p.905-909.

Kattis, S., Beskos, D., Cheng, A., 2003. 2D dynamic response of unlined and lined tunnels in poroelastic soil to harmonic body waves. *Earthquake engineering & structural dynamics*,v. 32, p.97-110.

Lee, V.W., Trifunac, M.D., 1979. Response of tunnels to incident SH-waves. *Journal of the Engineering Mechanics Division*, v. 105, p.643-659.

Martin, P., 1992. Boundary integral equations for the scattering of elastic waves by elastic inclusions with thin interface layers. *Journal of nondestructive evaluation* ,v.11, p.167-174.

Moore, I.D., Guan, F., 1996. Three-dimensional dynamic response of lined tunnels due to incident seismic waves. *Earthquake engineering & structural dynamics*,v. 25, p.357-369.

Murty, G.S., 1975. A theoretical model for the attenuation and dispersion of Stoneley waves at the loosely bonded interface of elastic half spaces. *Physics of the Earth and Planetary Interiors*,v. 11, p.65-79.

Newmark, N.M., Siess, C.P., Viest, I., 1951. Tests and analysis of composite beams with incomplete interaction. *Proc. Soc. Exp. Stress Anal* ,v.9, p.75-92.

Pao, Y.-H., Mow, C.-C., 1973. *Diffraction of Elastic Waves and Dynamic Stress Concentrations*, Crane, Russak & Co. Inc, New York. 694p.

Paskaramoorthy, R., Datta, S., Shah, A., 1988. Effect of interface layers on scattering of elastic waves. J*ournal of applied mechanics*,v. 55, p.871-878.

Rajabi, M., Hasheminejad, S.M., 2009. Acoustic resonance scattering from a multilayered cylindrical shell with imperfect bonding. *Ultrasonics*,v.49, p.682-695.

Rokhlin, S., Wang, Y., 1991. Analysis of boundary conditions for elastic wave interaction with an interface between two solids. *The Journal of the Acoustical Society of America*,v. 89, p.503-515.

Shen, H., Schiavone, P., Ru, C., Mioduchowski, A., 2001. Stress analysis of an elliptic inclusion with imperfect interface in plane elasticity. J*ournal of elasticity and the physical science of solids* ,v.62, p.25-46.

Shi, S., Han, F., Wang, Z., Liu, D., 1996. The interaction

of plane SH-waves and non-circular cavity surfaced with lining in anisotropic media. *Applied Mathematics and Mechanics*,v. 17, p.855-867.

Sudak, L., Ru, C., Schiavone, P., Mioduchowski, A., 1999. A circular inclusion with inhomogeneously imperfect interface in plane elasticity. *Journal of elasticity*,v.55, p.19-41.

Valier-Brasier, T., Dehoux, T., Audoin, B., 2012. Scaled behavior of interface waves at an imperfect solid-solid interface. *Journal of Applied Physics*,v.112, p.024904-024912.

Wang, X., Sudak, L., 2007. Scattering of elastic waves by multiple elastic circular cylinders with imperfect interface. *Waves in Random and Complex Media*,v.17, p.159-187.

Wang, Y., Yu, G., Zhang, Z., Feng, Y., 2000. Review on elastic wave propagation under complex interface (interface layer) conditions . *Advances in Mechanics*,v. 30,p.378- 390.